Using spacecraft measurements ahead of Earth in the Parker spiral to improve terrestrial space weather forecasts

D. L. Turner[1,2] and X. Li[1,2]

Received 21 September 2010; revised 11 November 2010; accepted 17 November 2010; published 8 January 2011.

[1] Space weather forecasting is important for mitigating the risks that the effects of the near-Earth space environment have on man-made systems. Here we investigate an innovative technique for extending the temporal range of solar wind–based forecast models by using solar wind measurements made azimuthally ahead of Earth in the Parker spiral near 1 AU. Cross correlations between STEREO (near 1 AU) and ACE (at L1) solar wind quantities are examined for a 1 year period during the most recent solar minimum, and we show that data from STEREO-B, which is azimuthally behind Earth in its orbit but ahead of Earth in the Parker spiral, can be used as an input to a relativistic electron forecast model to extend its capability to +6 days from its original range of +2 days. We show that this extended forecast performs better than simple persistence or average models for all 6 forecast days. We also compare +1 day solar wind speed forecasts using offset STEREO-B data and the Wang-Sheeley-Arge model, and we find that the offset STEREO-B data performs significantly better for estimating the future solar wind at Earth during the investigation period. We conclude that this technique could be particularly beneficial to space weather forecasting and argue for a permanent solar wind monitor at the fifth Lagrange point in the Sun-Earth system.

Citation: Turner, D. L., and X. Li (2011), Using spacecraft measurements ahead of Earth in the Parker spiral to improve terrestrial space weather forecasts, *Space Weather*, *9*, S01002, doi:10.1029/2010SW000627.

1. Introduction

[2] Since Richard C. Carrington noted the cause and effect of a large solar flare and subsequent geomagnetic storm in September of 1859, we have understood that there is a connection between solar events and Earth's magnetic field. In recognition of this, solar rotations, which occur on a ~27 day period as observed from Earth, are referred to as "Carrington" rotations. However, it was not until nearly a century later that L. Biermann proposed that there is a continuous outflow of plasma from the Sun, that is a continuum of charged particles and magnetic fields blowing outward in some solar wind (see history in the work by *Gosling* [2007]). *Parker* [1958] revolutionized our understanding of space weather and the solar-magnetospheric connection with his formulation of a model for the Sun's corona that included a continually expanding solar atmosphere. We now have developed a much better understanding of the solar wind from a multitude of in situ observations and improved modeling [*Gosling*, 2007]. The mean solar wind density, temperature, and velocity at 1 AU are 8.7 cm^{-3}, 12 × 10^5 K, and 468 km/s, respectively, with the velocity primarily in the radial direction away from the Sun. Since the solar wind plasma is an excellent conductor, the Sun's magnetic field is "frozen" into it as it radiates outward. This combined with the solar rotation leads to a spiral configuration of the interplanetary magnetic field (IMF) when viewed in the solar equatorial plane (see Figure 1 from *Gosling* [2007]), much like the spiral made by a person spinning and spraying a garden hose as viewed from above. In the solar wind, this IMF configuration is referred to as the Parker spiral. However, this is an idealized picture, as the solar wind is a turbulent plasma and highly variable. At any point, its conditions are the result of dynamics on the solar surface and in the corona when it originated as well as ongoing interactions with the solar wind around it.

[3] Space weather at the Earth can seriously affect man-made systems, from power grids to spacecraft [*Baker*, 2001], and changes in this "weather" are largely driven by changes in the solar wind. Thus, solar wind quantities are important for various space weather forecast models, which are used to mitigate the risk of space weather effects

[1]Laboratory for Atmospheric and Space Physics and Department of Aerospace Engineering Sciences, University of Colorado at Boulder, Boulder, Colorado, USA.
[2]Laboratory for Space Weather, Chinese Academy of Sciences, Beijing, China.

on man-made systems. For example, trapped energetic particles in the radiation belts pose a threat to spacecraft electronic components and have been known to critically affect satellite operations [e.g., *Baker et al.*, 1998]. Flux variations for these particles in the outer radiation belt are known to be correlated with the solar wind velocity [*Williams*, 1966; *Paulikas and Blake*, 1979; *Baker et al.*, 1979], and several radiation belt models are reliant on solar wind quantities as input [e.g., *Baker et al.*, 1990; *Li et al.*, 2001; *Li*, 2004; *Barker et al.*, 2005; *Fok et al.*, 2008] (for the *Li* [2004] real-time forecast, please see Web site: http://lasp.colorado.edu/~lix/). However, these models are limited in their effective forecast range by accurate solar wind forecast capabilities.

[4] Here we investigate a technique to estimate future solar wind conditions at Earth. This technique was first proposed, theoretically modeled, and discussed by *Yeh* [1984], and it simply relies on the nature of the solar wind, with its radial outward flow and IMF Parker spiral. We test the hypothesis that a spacecraft measurement of the solar wind taken azimuthally behind Earth in its orbit around the Sun, which is actually ahead of Earth in the Parker spiral, can be used to estimate the solar wind at some later time at Earth taking into account the solar rotation and azimuthal difference between the spacecraft and Earth. We examine the cross correlations between solar wind quantities observed at different azimuthal locations near 1 AU. The application to extending space weather forecasts is tested using a relativistic electron forecast model for Earth's outer radiation belt. Overall, we find this technique is applicable to extending some solar wind–based space weather forecasts, and we note the technique and analysis limitations.

2. Data Description

[5] The Advance Composition Explorer (ACE) mission was launched 25 August 1997, and since that time, it has provided measurements of the upstream solar wind from the first Lagrange (L1) point in the Sun-Earth system [*Stone et al.*, 1998]. Here, we use data from ACE's SWE-PAM (solar wind plasma) and MAG (magnetic fields) instruments for solar wind velocity, density, and magnetic field quantities. Also currently active in the solar wind is the Solar Terrestrial Relations Observatory (STEREO) mission [*Kaiser*, 2005], which launched its twin spacecraft on 25 October 2006. The STEREO mission involves two identical spacecraft, one ahead and one behind Earth in its orbit around the Sun. Figure 1 shows the locations of the STEREO-A (ST-A; for "Ahead") and STEREO-B (ST-B; for "Behind") on 29 August 2008 and 28 August 2009, which mark the start and stop times for the period used for most of this study. In this fixed heliographic-Earth-ecliptic (HEE) reference frame, the STEREO spacecraft will continue to travel away from Earth in their respective orbits until they each cross the X-Z plane on the other side of the Sun sometime in early 2015. For this study, we employ STEREO solar wind plasma, magnetic field, and ephemeris data available from NASA's CDAWeb (courtesy of Natasha Papitashvili at NASA/GSFC). Plasma data is from the PLASTIC instrument, which measures the plasma characteristics of solar wind protons, alphas, and heavier ions. STEREO magnetic fields are from the boom-mounted magnetometer (MAG) experiment that is part of the IMPACT instrument suite. We use hourly merged data from STEREO as available from CDAWeb and 10 minute ACE data, which is hourly averaged to align it with the STEREO data.

[6] For the outer radiation belt forecast model used to test the method described in this paper, we employ relativistic electron data from the GOES 11 spacecraft from NOAA's Geostationary Operational Environment Satellites series. GOES spacecraft have provided integral fluxes of relativistic electrons at geosynchronous orbit (GEO) for close to three decades. Until the latest generation, the GOES spacecraft since GOES 8 (including GOES 11) used the Energetic Particle Sensors (EPS) to measure electrons in three integral flux channels: >600 keV, >2 MeV and >4 MeV [*Onsager et al.*, 1996]. Here, we use daily averaged >2 MeV electron flux data from GOES 11.

3. Correlating Solar Wind Measurements From Different Locations

[7] Using the hourly, aligned ST-B and ACE data, we examine the cross correlations for various solar wind quantities measured by each spacecraft. Cross correlation (CC) is the measure of the similarity between two data sets given a time lag applied to one of them, and it is analogous to the linear correlation. Table 1 shows the cross correlations for the solar wind speed (V), density (n), and magnetic field components and magnitude as measured by the two spacecraft. The time offsets shown correspond to the amount of hours that the ST-B data is shifted ahead to produce the correlations shown. For the magnetic fields, we have simply compared the ACE fields in the GSM frame to the ST-B fields in the radial-tangential-normal (RTN) frame. In the RTN frame, the radial component is along the vector from the center of the Sun through the center of ST-B, the tangential component is the normalized cross product between the Sun's spin vector and the R direction, and the normal component completes the right-handed orthonormal system (i.e., it is along the projection of the solar north pole onto the plane normal to the R direction). With this in mind, we only compare the field components from each spacecraft that best correspond between the two coordinate systems.

[8] Table 1 reveals the strongest correlation (CC = 0.66) for the solar wind speed when the ST-B data is offset by 71 h. The solar wind density is less correlated at CC = 0.21, and the offset to achieve this CC is slightly longer at 75 h. The magnetic field components are very poorly correlated between the two spacecraft. This is expected considering they are in different reference frames and the variability in the IMF resulting from the solar wind's turbulent nature and ever-changing microscale conditions at the Sun (e.g.,

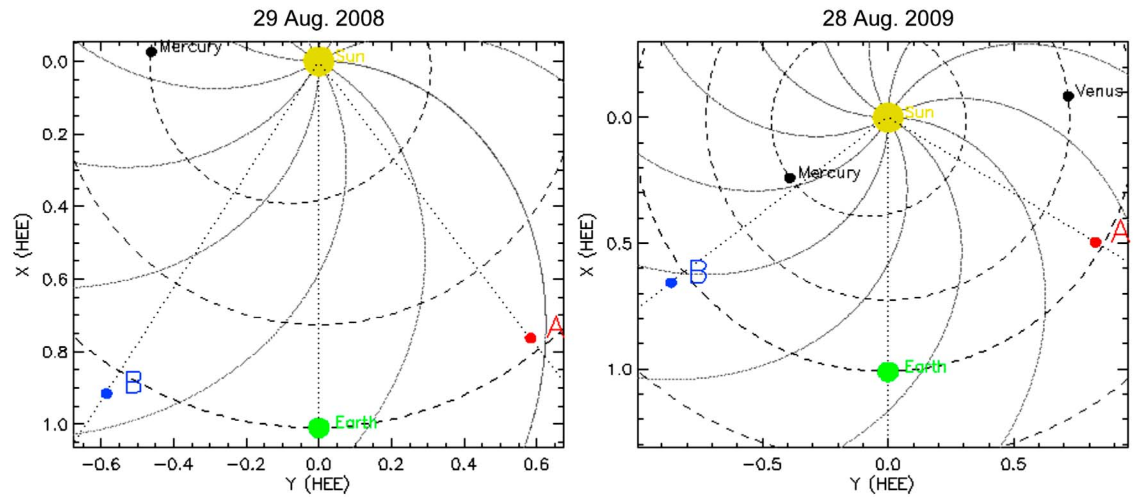

Figure 1. STEREO locations at 1200 UT on (left) 29 August 2008 and (right) 28 August 2009. ST-A (A) and ST-B (B) are shown ahead of and behind Earth in its orbit around the Sun (planetary orbits are indicated with the dashed lines). The Parker spiral and the orbits of Venus and Mercury are also shown. Distances in the heliographic-Earth-ecliptic (HEE) X-Y plane are given in units of AU. Note that the scales are different on the two plots. STEREO orbit plots are generated by the online Web tool at http://stereo-ssc.nascom.nasa.gov/where/.

magnetic field loops and arcades). However, the strong correlation in the speed is notable. Figure 2 shows the ST-B and ACE solar wind speed data for the period used in this study. Here, the full year of hourly data used to determine the cross correlations is shown, and the time offset between similar features is clearly evident. This offset corresponds to features originating from approximately the same macroscale features on the Sun (e.g., coronal holes) measured at different times by each spacecraft given the time it takes for the solar rotation to cover the angular distance between the two spacecraft. In this work, we focus primarily on the solar wind speed correlation.

[9] As Figure 1 shows, the STEREO spacecraft are continually moving away from Earth in the HEE frame. Because of this, the time offset between similar features measured by ST-B and ACE are continually changing (i.e., getting longer) throughout the period used for this study. For example, if only two months from the beginning of this time period are used (29 August to 28 October 2008), the CC and offset time for solar wind speed are 0.87 and 53 h, respectively. When only the last two months of the period are used (29 June to 28 August 2009), the CC and offset time for the solar wind speed are 0.56 and 108 h. So, for the solar wind speed, the correlation decreases and the time offset increases as the separation in the solar wind between the two spacecraft increases. This result is as expected.

Table 1. Cross Correlations for ST-B and ACE Solar Wind Quantities From 29 August 2008 to 28 August 2009[a]

Quantity	Cross Correlation	T Off (h)
V_{sw}	0.66	71
n_{sw}	0.21	75
B_{Tot}	0.06	119
B_z-B_n	0.04	94
B_y-B_t	–0.09	0
B_x-B_r	–0.16	1

[a]Time offsets (T off) corresponding to the cross correlations for each quantity are shown in hours.

[10] We also compare ST-B to ST-A data to determine how the correlations and offset times are affected by larger azimuthal separations. For the last two months of the period when the spacecraft are separated by around 110° in azimuth (see Figure 1), the CC and offset for solar wind speed are 0.36 and 196 h. Interestingly, the correlation for the B-normal component is still positive (CC = 0.11), and the density is actually more correlated than for the full period with the ST-B and ACE comparison (CC = 0.23). For the full time period comparing both ST-A and ST-B measurements, the CC and time offset for the solar wind speed are 0.46 and 138 h, respectively.

[11] This analysis reveals that a cross correlation does exist for the solar wind velocity as measured by two spacecraft separated in azimuth in the Parker spiral. Thus, it should be possible to use measurements from a spacecraft ahead of Earth in the Parker spiral (i.e., behind Earth in its orbit around the Sun) to extend forecasts that rely on solar wind velocity as an input. In section 4, we test this concept using ST-B data with a time offset as input to a solar wind–based forecast model of relativistic electron fluxes at GEO.

4. Extending a Radiation Belt Forecast

[12] To test this concept of using solar wind measurements from a spacecraft ahead of Earth in the Parker spiral

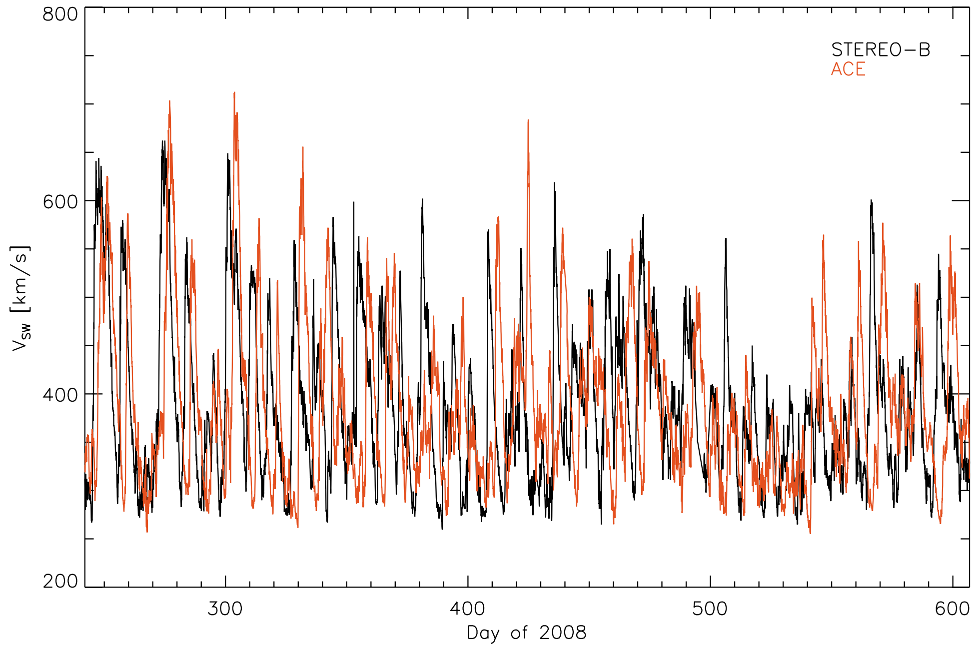

Figure 2. STEREO-B (black) and ACE (red) hourly solar wind speeds for 29 August 2008 to 28 August 2009.

to extend terrestrial space weather forecasts, we employ the *Li* [2004] model. *Li* [2004] described a forecast model for relativistic electron (>2 MeV) flux at GEO that uses solar wind speed and GOES >2 MeV daily averaged fluxes as inputs. The model has been shown to consistently outperform a simple persistence model (where tomorrow's flux is the same as today's) throughout the entire solar cycle for 1 and 2 day forecasts [*Turner and Li*, 2008]. However, it is limited in its forecast range by accurate solar wind forecasting capabilities.

[13] Taking advantage of the cross correlation in solar wind speed between ST-B and ACE, we use offset ST-B data as solar wind input to the *Li* [2004] model to see how well it performs for 3, 4, 5, and 6 day forecasts. Since the model already uses today's solar wind data from ACE to forecast 2 days into the future, it should be possible to use offset ST-B data, with its position ahead of Earth in the Parker spiral and temporal offset around 3 days ahead of ACE, to extend the forecast by several days. When the forecast model is run on its own using ACE and GOES 11 input data for 29 August 2008 to 28 August 2009, it achieves a prediction efficiency (PE) of 0.87 and 0.70 for the 1 and 2 day forecasts. For comparison, the PEs using the simple persistence model for 1 and 2 days are 0.81 and 0.56, respectively. PE is a measure of a forecast's performance, where PE = 1 represents a perfect forecast, PE = 0 represents an "average" model in which the forecast is the same as using the average value from the measured data, and PE < 0 means the model performs worse than the average model (see discussion on PE in the work by *Li* [2004]). The equation for PE is shown in equation (1), where m_i is the ith quantity of the measured data set, with $\langle m_i \rangle$ the set's average, and p_i is the ith quantity of the predicted (i.e., forecast) set.

$$PE = 1 - \frac{\sum_{i=1}^{N} (m_i - p_i)^2}{\sum_{i=1}^{N} (m_i - \langle m_i \rangle)^2} \tag{1}$$

[14] When ST-B velocity data are used as input to the model with no time shift applied, the PEs are 0.76 and 0.39 for the 1 and 2 day forecasts. However, when the ST-B data is shifted 3.5 days (84 h) forward in time and used as input, the PEs are improved to 0.84 and 0.61, which is closer to those achieved using the ACE data and both better than the simple persistence model. The shifting time was chosen based on the forecast model performance (i.e., it resulted in the highest PE for the period of August 2008 to August 2009). Based on this, we use the ST-B data with a 1.5 day offset to extend the *Li* [2004] model for 3 and 4 day forecasts and the ST-B data with no offset for 5 and 6 day forecasts. Figures 3 and 4 show the model results for the day 1 through day 6 forecasts. The model PEs are also displayed alongside the PEs from the simple persistence model for each day. Note that the model consistently outperforms simple persistence out to +6 days. In fact, by day 6, the persistence model performs poorer than just using the average GOES 11 flux, while the *Li* [2004] model with ST-B data still has a positive PE. The 27 day recurrence model PE for the same time period is −0.26, so the

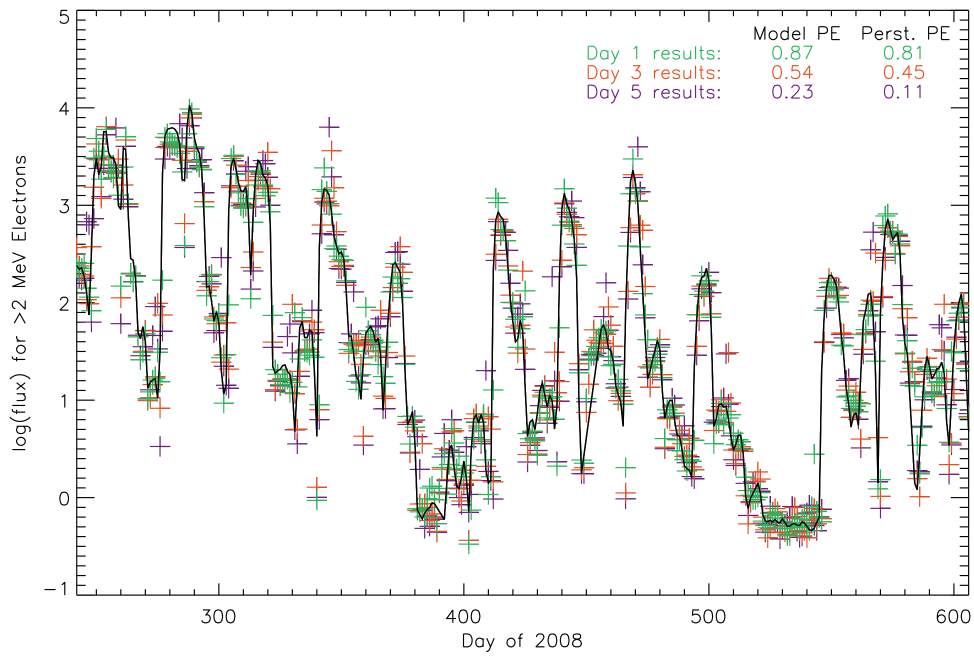

Figure 3. Results from the [*Li* 2004] model for 1, 3, and 5 day forecasts using ACE and ST-B data as solar wind inputs. Model forecasts are shown with different color crosses, and the observed GOES 11 daily average data is shown with the solid curve. Model and persistence PEs are also shown in the legend.

ST-B technique provides a very significant improvement over this too out to at least +6 days.

5. Discussion

[15] In this paper, we have addressed the following question: can solar wind measurements from a spacecraft that is azimuthally ahead of Earth in the Parker spiral be used to extend terrestrial space weather forecasts during periods of quasi-steady solar wind conditions? For a 1 year period during the most previous solar minimum, we have examined the cross correlations between the STEREO spacecraft, which are ahead and behind Earth in its orbit around the Sun, and ACE, which is upstream of Earth in the solar wind at the L1 point. Being behind Earth, ST-B is actually ahead of Earth in the Parker spiral and thus observes similar features in the solar wind several days ahead of ACE and ST-A. The quantity with the strongest correlation of those examined during the period 29 August 2008 to 28 August 2009 is the solar wind speed, with CC = 0.66 for an offset of 71 h applied to the ST-B data and compared with ACE. We have gone on to show that a space weather forecast, namely the *Li* [2004] relativistic electron forecast for GEO, can be successfully extended by using ST-B data as input. The model forecast range has been extended by a factor of three, from the original +2 day capability to +6 days. This is clear and simple proof of concept that solar wind data measured from ahead of Earth in the Parker spiral can indeed be used to extend terrestrial space weather forecasts that rely on solar wind data as input.

[16] We have also performed a simple comparison between the forecasting capabilities of offset ST-B data to the Wang-Sheeley-Arge (WSA) model for 1 day solar wind speed forecasting. We used the period from 15 March to 15 September 2008 and evaluated the performance using the PE for each speed forecast compared to ACE data. During this period, we simply offset the ST-B data by 40 h to serve as the forecast to compare with ACE. When compared to the 1 day WSA solar wind speed forecast, the offset ST-B data performs much better, achieving a PE of 0.71 compared to the WSA PE of 0.23. It is important to note, however, that the WSA 3 day forecast may be more accurate than the 1 day because of how the model's forecast is calculated [*Owens et al.*, 2005],though a thorough comparison of the WSA model compared to the time-shifted ST-B data is beyond the scope of this paper.

[17] There are some limitations that should be noted. This technique is particularly useful for approximating when we will encounter high-speed solar wind streams (HSSs) here at Earth. This is because of the nature of HSS origins from the Sun itself; they emanate from coronal holes, which are large-scale features that rotate with the Sun. Coronal mass ejections (CMEs), however, are explosive events whose arrivals at Earth cannot be approximated in the same manner (more on this below). Also, this study was conducted during a very quiet and extended solar minimum period. We expect that the correlations

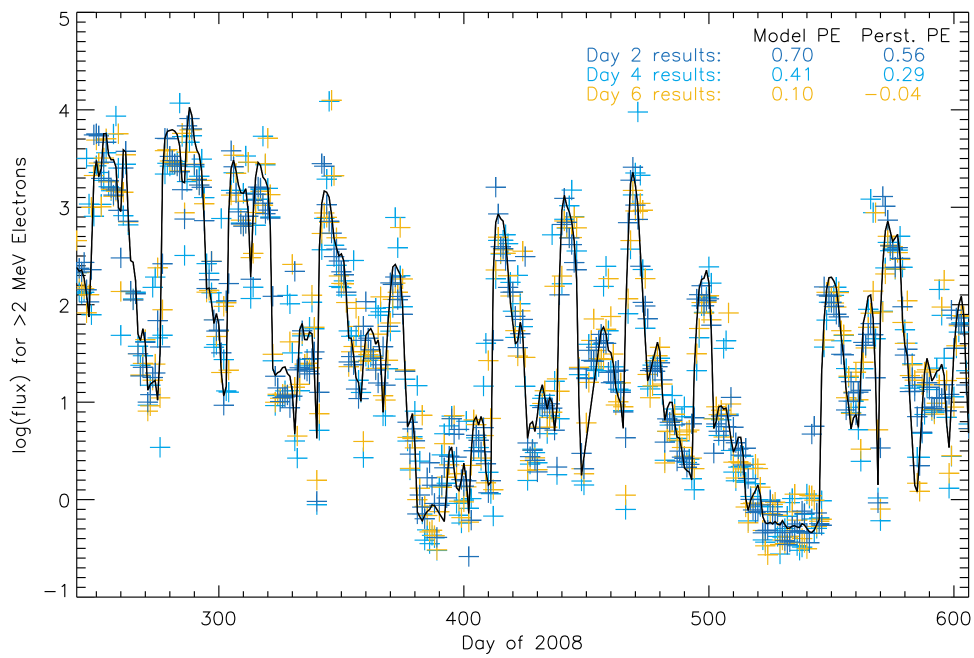

Figure 4. Results from the [*Li* 2004] model for 2, 4, and 6 day forecasts using ACE and ST-B data as solar wind inputs. Model forecasts are shown with different color crosses, and the observed GOES 11 daily average data is shown with the solid curve. Model and persistence PEs are also shown in the legend.

examined in this study will be weaker during solar maximum due to the increased activity in the solar wind and on the Sun itself. Thus, the performances of extended forecasts employing this technique will most likely also degrade significantly with enhanced solar activity, when impulsive events such as CMEs, solar flares, interplanetary shocks, and strong CIRs are more common features in the solar wind.

[18] Concerning any immediate application of this technique, there is an issue with the STEREO orbits. ST-B continues to drift in azimuth away from the Earth, as its orbital period is just slightly longer than that of the Earth. Thus, the performance of any model that uses ST-B data to extend its forecast time will continue to degrade as the correlation between the solar wind speed at ST-B and Earth decreases. If the spacecraft are still operational after early 2015, ST-A and ST-B will cross behind the Sun from Earth's perspective, and ST-A will then drift azimuthally toward Earth and ahead of it in the Parker spiral. However, there is a better solution to maintaining this solar wind forecasting capability: a solar wind monitor located at the fifth Lagrange point (L5). L5 is a stable orbital point and is located 60° behind Earth in azimuth along its orbit [*Vallado*, 2001]. ST-B passes closest to this location on 25 October 2009, after the period used for this study. We have compared ST-B and ACE data during a two month period centered around this date (i.e., 25 September 2009 to 25 November 2009), and the CCs and time offsets are 0.50 and 114 h for solar wind velocity and 0.04 and 115 h for density during this period. Thus, a spacecraft at the L5 point can provide a several day forecast extension capability for space weather models that rely primarily on solar wind velocity. A devoted L5 solar monitor would also provide several days warning of HSSs and, when combined with another solar wind monitor at the L1 point, a fixed stereoscopic view of the Sun. Such stereoscopic view is important, for example, for identifying whether halo CMEs are traveling toward or away from the Earth [e.g., *Kaiser*, 2005], so the space weather benefits of a solar wind monitor at L5 would go beyond the application to forecast extensions.

[19] Given its current location, ST-B can still be used for solar wind forecasting. Based on the comparison with ST-A, the correlations with the solar wind velocity and density (to a lesser extent) persist over large azimuthal separations (the velocity CC was 0.36 with 196 h offset for around 110° of separation). The correlations for the IMF are consistently weak, as is expected, and a forecast model with a strong IMF dependence would probably perform poorly if extended using the technique discussed here. For the forecast extension example discussed here, the forecast model has no dependence on IMF, which makes it ideal for use with this technique. However, if a model has only a weak dependence on the IMF, we speculate that the ST-B IMF measurements may suffice as an estimate. For a real-time forecast, access to real-time ST-B data is necessary, and such data from the STEREO spacecraft are indeed available from the mission space weather beacon (see

http://stereo-ssc.nascom.nasa.gov/beacon/beacon_insitu.shtml). Such data can be used to extend space weather forecasts or any other real-time models that rely on solar wind velocity, like electron flux mapping around GEO using statistical asynchronous regression for example (e.g., D. L. Turner et al., An improved forecast system for relativistic electrons at geosynchronous orbit, submitted to *Space Weather*, 2010).

6. Conclusions

[20] We have shown how solar wind velocity measurements from spacecraft that are azimuthally ahead of Earth in the Parker spiral (behind it in its orbit around the Sun) can be used to accurately predict the solar wind speed at Earth several days later. This concept, which was originally proposed by *Yeh* [1984], can be used for extending space weather forecasts that rely on solar wind data, as we have shown here by extending the *Li* [2004] relativistic electron forecast to +6 days. This presents a good argument for a devoted solar wind monitor at the stable L5 point in the Sun-Earth system. Such a monitor would be beneficial to solar and solar wind physics in general, as STEREO is currently proving. Concerning some additional space weather benefits, a solar wind monitor at L5 would provide several days warning for HSSs and could be useful for coronograph imaging, which *Sun et al.* [2008] showed can be used for space weather forecasting applications.

[21] **Acknowledgments.** The authors would like to thank Peter MacNeice at NASA's CCMC for providing the 1 day Wang-Sheeley-Arge solar wind velocity forecast data. This work was supported by NSF grants (ATM-0842388 and ATM-0902813) and also by grants from the National Natural Science Foundation of China (40621003 and 40728005).

References

Baker, D. (2001), Satellite anomalies due to space storms, in *Space Storms and Space Weather Hazards*, edited by I. A. Daglis, chap. 10, pp. 251–284, Springer, New York.

Baker, D. N., R. D. Belian, P. R. Higbie, and E. W. Hones (1979), High-energy magnetospheric protons and their dependence on geomagnetic and interplanetary conditions, *J. Geophys. Res.*, *84*(A12), 7138–7154.

Baker, D. N., R. L. McPherron, T. E. Cayton, and R. W. Kebesadel (1990), Linear prediction filter analysis of relativistic electron properties at 6.6 R_E, *J. Geophys. Res.*, *95*(A9), 15,133–15,140.

Baker, D. N., J. H. Allen, S. G. Kanekal, and G. D. Reeves (1998), Disturbed space environment may have been related to pager satellite failure, *Eos Trans. AGU*, *79*(40), 477.

Barker, A. B., X. Li, and R. S. Selesnick (2005), Modeling the radiation belt electrons with radial diffusion driven by the solar wind, *Space Weather*, *3*, S10003, doi:10.1029/2004SW000118.

Fok, M.-C., R. B. Horne, N. P. Meredith, and S. A. Glauert (2008), Radiation Belt Environment model: Application to space weather nowcasting, *J. Geophys. Res.*, *113*, A03S08, doi:10.1029/2007JA012558.

Gosling, J. T. (2007), The solar wind, in *Encyclopedia of the Solar System*, 2nd ed., edited by L.-A. McFadden, P. R. Weissman, and T. V. Johnson, pp. 99–116, Academic, San Diego, Calif.

Kaiser, M. L. (2005), The STEREO mission: An overview, *Adv. Space Res.*, *36*, 1483–1488.

Li, X. (2004), Variations of 0.7–6.0 MeV electrons at geosynchronous orbit as a function of solar wind, *Space Weather*, *2*, S03006, doi:10.1029/2003SW000017.

Li, X., M. Temerin, D. N. Baker, G. D. Reeves, and D. Larson (2001), Quantitative prediction of radiation belt electrons at geostationary orbit based on solar wind measurements, *Geophys. Res. Lett.*, *28*(9), 1887–1890.

Onsager, T. G., et al. (1996), Operational uses of the GOES energetic particle detectors, in *GOES-8 and Beyond*, edited by E. R. Washwell, *Proc. SPIE Int. Soc. Opt. Eng.*, 2812, 281–290, doi:10.1117/12.254075.

Owens, M. J., C. N. Arge, H. E. Spence, and A. Pembroke (2005), An event-based approach to validating solar wind speed predictions: High-speed enhancements in the Wang-Sheeley-Arge model, *J. Geophys. Res.*, *110*, A12105, doi:10.1029/2005JA011343.

Parker, E. N. (1958), Dynamics of the interplanetary gas and magnetic fields, *Astrophys. J.*, *128*, 664–676.

Paulikas, G. A., and J. B. Blake (1979), Effects of the solar wind on magnetospheric dynamics: Energetic electrons at the synchronous orbit, in *Quantitative Modeling of Magnetospheric Processes*, *Geophys. Monogr. Ser.*, vol. 21, edited by W. P. Olsen, pp. 180–202, AGU, Washington, D. C.

Stone, E. C., A. M. Frandsen, R. A. Mewaldt, E. R. Christian, D. Margolies, J. F. Ormes, and F. Snow (1998), The Advanced Composition Explorer, *Space Sci. Rev.*, *86*, 1–22.

Sun, W., C. S. Deehr, M. Dryer, C. D. Fry, Z. K. Smith, and S.-I. Akasofu (2008), Simulated Solar Mass Ejection Imager and "Solar Terrestrial Relations Observatory-like" views of the solar wind following the solar flares of 27–29 May 2003, *Space Weather*, *6*, S03006doi:10.1029/2006SW000298.

Turner, D. L., and X. Li (2008), Quantitative forecast of relativistic electron flux at geosynchronous orbit based on low-energy electron flux, *Space Weather*, *6*, S05005, doi:10.1029/2007SW000354.

Vallado, D. A. (2001), *Fundamentals of Astrodynamics and Applications*, 2nd ed., Kluwer Acad., Dordrecht, Netherlands.

Williams, D. J. (1966), A 27-day periodicity in outer zone trapped electron intensities, *J. Geophys. Res.*, *71*(7), 1815–1826.

Yeh, T. (1984), A hydromagnetic model of corotating conductive solar wind streams, *Astrophys. Space Sci.*, *98*, 353–366.

X. Li and D. L. Turner, Laboratory for Atmospheric and Space Physics, University of Colorado at Boulder, 1234 Innovation Dr., Boulder, CO 80303, USA. (drew.lawson.turner@gmail.com)